Available online at www.sciencedirect.com
SCIENCE DIRECT
European Journal of Pharmacology 540 (2006) 34–45
www.elsevier.com/locate/ejphar

Transcriptional changes facilitate mitotic catastrophe in tumour cells that contain functional p53

Sylvia Mansilla [a], Waldemar Priebe [b], José Portugal [a,*]

[a] Instituto de Biología Molecular de Barcelona, CSIC, Parc Cientific de Barcelona, Josep Samitier, 1-5, E-08028 Barcelona, Spain
[b] The University of Texas M. D. Anderson Cancer Center, Houston, TX 77030, USA

Received 7 January 2006; received in revised form 4 April 2006; accepted 19 April 2006
Available online 30 April 2006

Abstract

Exposure of Jurkat T lymphocytes containing functional p53 to nanomolar concentrations of bisanthracycline WP631 resulted in arrest at the G_2/M checkpoint and transient senescence-like phenotype in the presence of DNA synthesis. The cells entered crisis, became polyploid, showed aberrant mitotic figures, and died through mitotic catastrophe. Cell death was accompanied by changes in the expression profile of various oncogenes and tumour suppressor genes including the down-regulation of *p53*. The changed expression was confirmed for some of these genes using semi-quantitative RT-PCR, and the decline in p53 protein levels was established. Our results suggest that WP631 induced changes in cell cycle control pathways leading to death of Jurkat T cells through mitotic catastrophe, which occurred in the absence of caspase-2 and caspase-3 activities, rather than apoptosis.

Keywords: Mitotic catastrophe; Transcriptome; WP631; Anthracycline; Jurkat T lymphocyte; p53

1. Introduction

A widespread model used to explain how chemotherapy works in the treatment of cancer considers that antitumour drugs induce cells to undergo apoptosis (programmed cell death) a phenomenon usually linked to the presence of functional p53. Cells that are resistant to apoptosis might therefore be resistant to therapy (Johnstone et al., 2002; Lowe et al., 1994; Perego et al., 2001). However, resistance to apoptotic induction alone is not sufficient for cell survival after treatment with antitumour drugs (Brown and Attardi, 2005; Brown and Wilson, 2003; Weller, 1998), implying that many drugs induce cell death through pathways other than p53-mediated apoptosis. While tumours of haematological origin, including T-cell lymphomas, and some solid tumours are often sensitive to the induction of apoptosis after treatment with DNA-binding drugs (Brown and Attardi, 2005; da Silva et al., 1996; Weller, 1998), for many solid tumours apoptosis might not be the main mediator of cell death (Brown and Attardi, 2005; Roninson et al., 2001; Weller, 1998; Zhivotovsky, 2004). For several antitumour drugs, it has been demonstrated that the mechanism of cell death may differ depending on the dose used, and it is often accompanied by changes in the profile of gene expression after treatment (Chang et al., 2002; Gatti et al., 2004; Mansilla et al., 2003; Roninson et al., 2001; Torres and Horwitz, 1998). In a recent review on solid tumours treated with radiotherapy, it was concluded that there is not clear evidence that the degree of apoptotic response, or p53 levels, are predictive of a solid tumour's response to therapy (Brown and Wilson, 2003).

The relationship between cell cycle arrest and apoptosis is well understood in the context of the role of p53 in the G_1 phase (Vogelstein et al., 2000). Nevertheless, the inhibition of apoptosis may be compensated by increasing the fraction of cells that suffer permanent growth arrest, with phenotypic features of cell senescence, or cells might die through mitotic catastrophe (Roninson et al., 2001). Regardless the functional status of the p53 protein, death following G_2 arrest has been observed in several cell types in the presence of DNA-damaging agents (Chang et al., 2002; Elmore et al., 2002; Eom et al., 2005; Minemoto et al., 2003; Sleiman and Stewart, 2000; Villamarín et al., 2002).

* Corresponding author. Tel.: +34 93 403 4959; fax: +34 93 403 4979.
E-mail address: jpmbmc@ibmb.csic.es (J. Portugal).

0014-2999/$ - see front matter © 2006 Elsevier B.V. All rights reserved.
doi:10.1016/j.ejphar.2006.04.035

Antitumour drugs can induce a senescence-like cell cycle arrest or 'accelerated senescence' (Brown and Attardi, 2005; Elmore et al., 2005; Shay and Roninson, 2004), which is largely considered p53-dependent (Chang et al., 1999; Roninson, 2002). 'Accelerated senescence', which resembles 'replicative senescence' (also called M1 stage) in human cells, results primarily from the progressive shortening of telomeres in cells that do not express sufficient telomerase activity to fully maintain the telomeres (Shay and Wright, 2005). In senescent cells, growth arrest is initiated by the activation of p53 (Roninson, 2003). In the absence of functional p53, cells bypass the M1 stage and telomeres continue to shorten until crisis (or M2 stage). M2 is characterized by the presence of DNA synthesis and cell death through mitotic catastrophe. Consequently, there is no proliferation because of a balance between cell division and death.

Mitotic catastrophe, which can be considered one form of p53-independent cell death, has been associated with DNA damaging drugs (Brown and Attardi, 2005; Eom et al., 2005; Huang et al., 2005; Roninson et al., 2001), and it has been reported in patients with de novo acute leukaemia after treatment (Yashige et al., 1999). However, there is no generally accepted definition of mitotic catastrophe (Brown and Attardi, 2005; Castedo et al., 2004a; Roninson et al., 2001), though it is characterized by a transient halt in the G_2/M phase followed by premature mitosis. From a morphological point of view, mitotic catastrophe is the result of abnormal mitosis, which can induce polyploidy (Nitta et al., 2004) and can end in the occurrence of large-multinucleated cells (Brown and Attardi, 2005; Roninson et al., 2001). Mitotic catastrophe can be regarded as a type of cell death that occurs during, or close to, the metaphase, or after a faulty mitosis with micronucleation (Castedo et al., 2004b; Chang et al., 2000). In some cell types, mitotic catastrophe can be accompanied by activation of caspases, which resembles the apoptotic cell death mechanisms (Bataller and Portugal, 2005; Castedo et al., 2004b; Mansilla et al., 2006; Sleiman et al., 1998), although activation of caspases is a frequent, but not sufficient, hallmark of apoptosis (Zhivotovsky, 2004). Nevertheless, whether caspase-dependent or independent, this mechanism is an important safeguard to prevent damaged cells from perpetuating, and diminishing the risk of aneuploidy in the daughter cells.

We have demonstrated that the response of Jurkat T lymphocytes to the anthracycline daunorubicin was clearly dose-dependent in cells containing functional p53 (Mansilla et al., 2003). The treatment of Jurkat T cells with the IC_{75} of daunorubicin resulted in almost immediate apoptosis, while decreasing the drug concentration to about the IC_{50} caused G_2 arrest and senescence with morphological aspects of apoptosis followed by necrosis after longer incubation periods. The time-dependent response of these cells was correlated with a different pattern of gene expression in cells undergoing immediate apoptosis (Mansilla et al., 2003).

The bisanthracycline WP631 is a DNA-binding agent that acts primarily as a potent inhibitor of Sp1-dependent transcription (Gaidarova and Jiménez, 2002; Inge et al., 2002; Mansilla et al., 2004; Martín et al., 1999; Qureshi et al., 2005; Villamarín et al., 2002). In breast cancer cells, it seems to circumvent some mechanisms of resistance, producing transient cell senescence and cell death through mitotic failure, leading to multinucleated cells (Mansilla et al., 2006). We hypothesized that WP631 induces cell death trough a p53-independent mechanism, and determined its effects on the levels of functional p53, together with variations in the whole transcriptome in Jurkat T lymphocytes.

2. Materials and methods

2.1. Cell line and culture conditions

Early-passage Jurkat T lymphocytes (American Type Culture Collection-TIB-152, clone E6-1, with no more than 3 serial subcultures after arrival) were maintained in RPMI 1640 medium (Gibco, Life Technologies, Prat de Llobregat, Spain) supplemented with 10% foetal bovine serum (Gibco), 100 U/ml penicillin, 100 μg/ml streptomycin, 2 mM L-glutamine (Gibco) and 2 mM Hepes (pH 7.4), at 37 °C in a humidified atmosphere with 5% CO_2.

WP631 (4-methylbenzyl-*N*-bis[daunorubicin]), synthesized as described previously (Chaires et al., 1997), and daunorubicin (Sigma, St. Louis, MO) were prepared as 500 μM solutions in sterile 150 mM NaCl and brought to the final concentration with RPMI 1640 medium just before use.

2.2. Grown inhibition assays and assessment of cell death

The effect of WP631 on Jurkat cells growth was determined by using the MTT dye (3-(4,5-dimethylthiazol-2-yl)-2,5-diphenyltetrazolium bromide) assay in 96-well microtiter plates with flat-bottomed wells (Corning Costar, Corning, NY) in a total volume of 100 μl. Cells subcultured at a density of 5×10^4 cells/ml were incubated with various concentrations of WP631 at 37 °C for 72 h. After incubation, MTT (Sigma, St. Louis, MO) was added to each culture (0.5 mg/ml, final concentration). The dark-coloured crystals produced by viable cells were solubilized with 30 mM HCl in 2-propanol. Absorbance was determined at 570 nm using a SPECTRAmax 250 microplate reader (Molecular Devices, Sunnyvale, CA).

To assess the capacity of WP631 to induce cell death, viable cell number was routinely determined in all the experiments using the exclusion of Trypan blue dye (Sigma) and a haemocytometer. Apoptosis was quantified and distinguished from necrosis by using the Annexin-V-Fluos staining kit (Roche Diagnostics, Mannheim, Germany) and flow cytometry (Vermes et al., 1995) using a Coulter Epics-XL flow cytometer (Coulter Corporation, Hialeah, FL).

2.3. Cell cycle distribution

After treatment with WP631, or daunorubicin, for various periods of time, Jurkat T cells were harvested, stained with propidium iodide (Sigma) and the nuclei were analyzed with a Coulter Epics-XL flow cytometer (Coulter Corporation), using the 488 nm line of an argon laser and standard optical emission

filters. Percentages of cells at each phase of the cell cycle were estimated from their DNA content histograms after drug treatment.

2.4. Senescence-associated β-galactosidase staining and DNA synthesis assays to detect senescent cells

After treatment with WP631, cells were fixed in 3% formaldehyde and stained with fresh senescence-associated β-galactosidase stain solution as described elsewhere (Dimri et al., 1995), using X-gal (5-bromo-4-chloro-3-indolyl β-D-galacto-pyranoside) at pH 6.0. Senescence-like growth arrest was determined as the percentage of senescence-associated β-galactosidase positive cells appraised by phase-contrast microscopy, after scoring 50–100 cells for each control and WP631-treated samples.

DNA synthesis was assayed as described elsewhere (Mansilla et al., 2003), utilizing BrdU (5′-Bromo-2′-deoxy-uridine), BrdU-detection kit III (Roche Diagnostics) and a colorimetric reaction using 4-Nitro blue tetrazolium chloride (Roche Diagnostics), measured at 370 nm.

2.5. Cytological characterization of cells undergoing mitotic catastrophe

A CompuCyte Laser Scanning Cytometer (CompuCyte; Cambridge, MA) was used for morphological observation of multinucleated cells. The presence of multinucleated cells was assessed on microscope slides containing Jurkat T cells prepared as described above for flow cytometry, and analyzed using a 40× objective and 5 mW of Argon laser power. Using the WinCyte 3.4 software (CompuCyte), a cell gallery was created by relocation of cells from each of the major peaks in the histogram of integrated red fluorescence. Polyploidy was determined by setting an appropriate histogram gate, while the morphology was established under the microscope. We deemed that enlarged cells containing multiple evenly stained nuclei (polyploid, multinucleated cells) underwent mitotic catastrophe (Lock and Stribinskiene, 1996; Roninson et al., 2001).

For the analysis of mitotic figures in WP631-treated cells, about 50–100 μl of cells in RPMI 1640 medium were dropped on clean slides with a Pasteur pipette and left to air-dry. Cells were fixed using Carnoy's solution (3 vol. methanol, 1 vol. glacial acetic acid). Slides were stained for 30 min with Leishman's stain (BDH, Poole, UK) diluted in methanol, and examined under a Carl-Zeiss Axiophot microscope.

2.6. Human array experimental design

The Human Oncogene/Tumor Suppressor Atlas Array (#634519, BD Biosciences Clontech, Palo Alto, CA) was used to monitor changes in the levels of transcription of 199 genes in Jurkat T lymphocytes, treated with 60 nM WP631 (its IC_{75} in Jurkat T cells determined after 72-h continuous treatment (Table 1)), compared with untreated cells. The annotated function for all these genes, as well as their accession number, can be found at the BD Biosciences homepage (http://www.clontech.com/clontech/atlas/genelists/index.shtml). 190 of these genes are commonly classified as oncogenes or tumour suppressor genes, while 9 are regarded as housekeeping genes.

Table 1
Evaluation of the cytotoxicity of WP631 in Jurkat T lymphocytes after 72 h of continuous treatment

	IC_{50} (nM)	IC_{75} (nM)
WP631	17.7±1.8	60.0±19.5

Data are mean±S.E.M., determined from six independent dose–response curves by the MTT-dye assay.

All the experiments were designed to conform to the guidelines provided by MIAME (http://www.mged.org/Workgroups/MIAME/miame.html). Experimental details are provided in the following paragraphs. A database consisting of the average raw data for all genes in the different experiments and the processed (normalized) results is available online at the Journal's web page.

2.7. RNA extraction, cDNA synthesis, and array hybridization

Total RNA was isolated from control cells (those to which no drug was added) and from cells treated with 60 nM WP631 (its IC_{75} in Jurkat T cells) after 4 h. The UltraspecRNA isolation reagent (Biotecx, Houston, TX) was used following the procedure provided by the vendor. RNA was digested with RNAse-free DNase I (Roche Diagnostics) in the presence of RNAse inhibitors (RNasin, Promega, Madison, WI), phenol extracted and precipitated. The pellet was dissolved in RNAse free water and the yield and purity of total RNA were assessed spectrophotometrically.

About 5 μg of RNA was used to convert total RNA into ^{32}P-labeled first-strand cDNA, using α-[^{32}P]-dATP and the gene specific CDS-primer mix for the Atlas array (BD Biosciences) following the protocol provided by the vendor. The labelled cDNA was purified from unincorporated α-[^{32}P]-dATP using a NucleoSpin Column (BD Biosciences).

Hybridization of the Human Oncogene/Tumor Suppressor Atlas Arrays (BD Biosciences Clontech) with the labelled probes were performed in triplicate, using ExpressHyb solution (BD Biosciences) at 68 °C for 16 h, and they were washed as described elsewhere (Mansilla et al., 2003) prior to their quantification.

2.8. Human array data analysis

The hybridized arrays were exposed to an Imaging Screen-K (Bio-Rad, Munich, Germany) and analyzed using a Molecular Imager FX (Bio-Rad). For image processing and quantification, the intensity of the radioactive signals on the different Human Oncogene/Tumor Suppressor Atlas Arrays was analyzed using Quantity One 4.1.1 software (Bio-Rad), and the peak areas were transferred into a standard spreadsheet program. To analyze the differential gene expression in the absence, and in the presence of WP631, the background in each array was subtracted of the spot values, and the average intensity of the housekeeping gene

GAPDH (glyceraldehyde-3-phosphate dehydrogenase), widely utilized as control in transcription experiments, was used to normalize the results and to adjust for differences in labelling and the quantities of RNA. All the experiments were undertaken in triplicate and the results averaged.

After normalization, data for each gene were calculated as the $\log_2$ of the expression ratio between 'WP631-treated' and 'control' membranes. A post-normalization cut-off of 2.5-fold increase or decrease in the expression ratio was used (see Results). There is no firm theoretical basis for selecting a particular level of significance, but normally a less stringent cut-off of two-fold increase or decrease is used.

2.9. Semi-quantitative reverse-transcriptase polymerase chain reaction (RT-PCR) and quantitative real-time PCR (qRT-PCR)

Changes in gene expression were verified by semi-quantitative RT-PCR using *GAPDH* as an internal normalization standard. Total RNA was isolated from control cells (no drug) and cells treated with WP631 after 4 h, and digested with DNaseI as described above. Sub-saturating RT-PCR conditions were adjusted to 10 ng of total RNA and 20–25 amplification cycles, with the annealing reactions carried out at 50 °C for 1 min, using the OneStep PCR kit (Qiagen, Hilden, Germany) following the manufacturer's instructions. The primers used (0.6 μM) were: mycdir, 5-AAAAAGCCACAGCATACATCC-3′, mycrev, 5′-TCTCAAGACTCAGCCAAGGTT-3′, p53dir, 5′-TCAGCATCTTATCCGAGTGG-3′, p53rev, 5′-CCTGGGCATCCTTGAGTTC-3 GAPDHdir, 5′-TCAGCCGCATCTTCTTTTG-3′, GAPDHrev, 5′-TGATGGCATGGACTGTGGT-3′. PCR samples were electrophoresed in a 2% agarose gel, stained with ethidium bromide and quantified using a Molecular Dynamics densitometer (Sunnyvale, CA).

For quantitative real-time PCR (qRT-PCR), RNA, obtained as in the previous paragraph, was used to prepare cDNA by a reverse transcription reaction of 60 min at 37 °C using oligo-dT and Omniscript Reverse Transcriptase (Qiagen). qRT-PCR was carried out with the Amplifluor Universal detection system (Intergen, Oxford, UK). The QRT-PCRs were set up with 10 ng cDNA and three oligonucleotides: 50 nM Amplifluor Uniprimer, fluorescein (Intergen), and a combination of 5 nM forward primer and 5 nM reverse primer. For $p21^{WAF1}$ detection, the primers used were: *p21forward*, 5′-ACTGAACCTGACCGTACACAGGGGACAGCAGAGGAAGAC-3′, *p21reverse*, 5′-CCGGCGTTTGGAGTGGTAG-3′. For GAPDH detection the primers were: GAPDHforward, 5′-ACTGAACCTGACCGTACAACAGCGACACCCACTCCTCCAC-3′, GAPDHreverse, 5′-CCGGCGTTTGGAGTGGTAG-3′. The forward primer is extended at the 5′-end with ACTGAACCTGACCGTACA, a sequence also part of the Amplifluor Uniprimer. The qRT-PCR reactions were initiated on an Opticon real-time PCR machine (MJ Research, Ecogen, Barcelona, Spain) by 10 min at 95 °C, followed by 50 PCR cycles of 15 s at 95 °C, 20 s at 55 °C, and 40 s at 72 °C. The relative amounts of cDNA present in the samples were calculated from the fluorescence increment due to primer extension above the threshold level, and the values obtained were represented as the folds of activation of the analyzed gene (which were proportional to the number of gene copies) in respect to those of the housekeeping GAPDH gene.

2.10. Western blot

Protein was extracted from WP631-treated and control cells, at the times indicated in Fig. 4C, with a lysis buffer consisting of 50 mM Tris–HCl (pH 8), 150 mM NaCl, 5 mM EDTA, 0.5% Nonidet P-40 and 0.1 mM phenylmethylsulphonyl fluoride, containing 2 μl/ml aprotinin and 1 μg/ml leupeptin. Total protein was quantified by the Bradford assay (Bio-Rad). About 30 μg of denatured proteins was subjected to electrophoresis on SDS-polyacrylamide gels, blotted onto Optitran BA-S85 membranes (Schleicher and Schuell, Dassel, Germany), probed with anti-$p21^{WAF1}$ (Calbiochem, VWR International, Barcelona, Spain), anti-p53 (Calbiochem), anti-Actin (Sigma) and anti-β-tubulin (Chemicon International, Temecula, CA) antibodies, and detected by chemiluminescence using Luminol (Sigma).

2.11. Quantitative detection of mRNA for the human telomerase catalytic subunit hTERT

A quantitative detection of hTERT mRNA was performed with the LightCycler *TeloTAGGGh*TERT quantification kit (Roche Diagnostics) and a LightCycler instrument for real-time PCR (Roche). Experiments were carried out following the manufacturer's instructions, using 200 ng of total RNA obtained from WP631-treated Jurkat T cells or from untreated cells, as described above. Quantification of mRNA encoding for porphobilinogen deaminase (PBGD) was processed for use as a reference for relative quantification.

2.12. Caspase activity assays

Caspase-3 and caspase-2 activities were quantified with the BD-ApoAlert Caspase-3 Colorimetric assay kit (BD Biosciences) and the Caspase-2/ICH-1 Colorimetric Protease assay kit (MBL, BioNova, Madrid, Spain), respectively, according to the manufacturer's instructions. The fold-increase in protease activity, which measures the proteolytic cleavage of the chromophore *p*NA (*p*-nitroanilide) from the labelled substrate, was obtained by comparison of the spectrophotometric readings at 405 nm of samples from drug-treated and untreated cells.

3. Results

3.1. Jurkat T lymphocytes undergo transient senescence, followed by crisis and mitotic catastrophe after treatment with nanomolar concentrations of WP631

The concentrations of WP631 assayed in Jurkat T cells corresponded to the IC_{50} and IC_{75} doses determined by the MTT assay after 72-h continuous treatment (Table 1). At both concentrations, the cells transiently accumulated in G_2/M, re-entered the cell cycle and eventually died, in a time-dependent

way, following the withdrawal of the drug. Thereby, most of the experiments described below were undertaken using the IC_{75} for WP631.

After 72-h continuous treatment, the WP631-induced arrest in G_2 (Fig. 1A) was accompanied by expression of the lysosomal senescence-associated β-galactosidase at pH 6 (right panels in Fig. 1A). Following the 72-h treatments, the cells treated with 18 nM (IC_{50}) WP631 survived up to 9 days in fresh, drug-free, medium, whereas cells treated with 60 nM (IC_{75}) WP631 survived in fresh medium up to 2 days, based on exclusion of Trypan blue dye by viable cells.

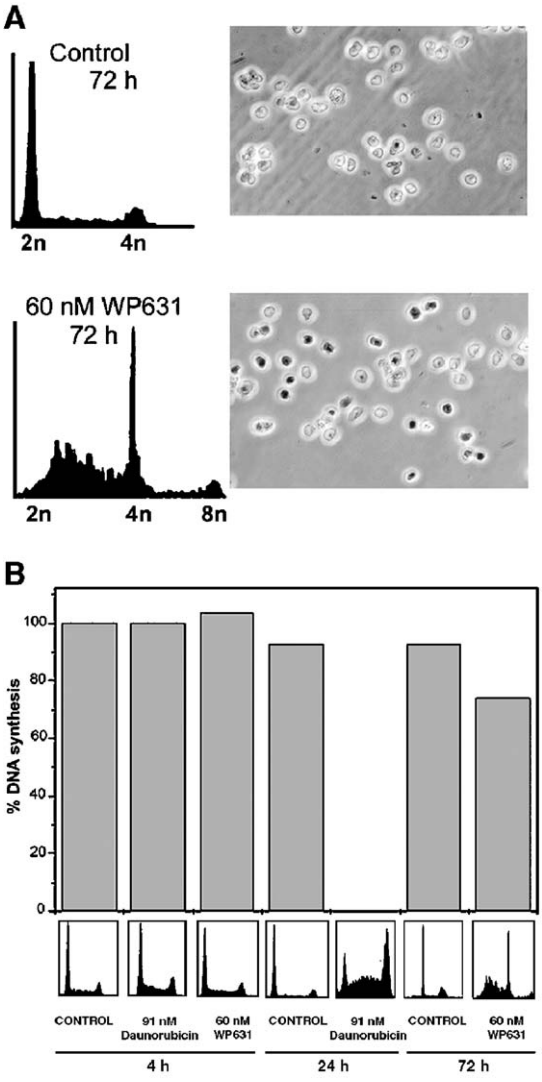

Fig. 1. Cell cycle distribution of Jurkat T lymphocytes treated with 60 nM WP631 (its IC_{75}) for 72 h. (A) Cell cycle distribution analyzed using propidium iodide and flow cytometry (left panel), and expression of senescence-associated β-galactosidase (pH 6.0) in control, untreated cells, and in cells treated with the drug (right panel). Note the presence of about 50% of positive-stained senescent cells after treatment with WP631 (originally photographed at 400× magnification). (B) Percentage of DNA synthesis in cells treated with WP631 compared with untreated and daunorubicin-treated cells. Values, which correspond to the average of two independent experiments, are presented with respect to the DNA synthesis determined in untreated cells, after 4 h. Unlike in daunorubicin-treated cells, cells treated with WP631 synthesized DNA significantly. The lower panel shows the cell cycle distribution of the cells tested for DNA synthesis.

A comparison of DNA synthesis and cell cycle distribution in the presence of WP631 or daunorubicin is displayed in Fig. 1B. After treatment with 60 nM WP631, Jurkat T cells arrested in G_2 and maintained their capacity for synthesizing DNA, reaching around 80% of the DNA synthesis levels observed in untreated cells (Fig. 1B). These cells underwent polyploidy, since 8*n* cells were observed after treatment with WP631 (Figs. 1A and 2A), in agreement with previous observations (Pozarowski et al., 2004; Villamarín et al., 2003). By contrast, DNA synthesis was abolished in the presence of daunorubicin from 24-h treatment onwards consistent with cell senescence (M1 stage) (Fig. 1B). Taken together, these results indicate that WP631-treated Jurkat T cells halt transiently in the G_2 phase of the cell cycle, while, in parallel, they maintained capacity for synthesizing DNA. When the drug was withdrawn, DNA synthesis continued, and the cells were directed to what has been designed as crisis or M2 stage (MacKenzie et al., 2000; Shay and Roninson, 2004), which ended in mitotic failure and cell death (see below).

3.2. Treatment with WP631 induces polyploidy in Jurkat T lymphocytes cells, which accumulate aberrant mitotic figures

To morphologically characterize if Jurkat T lymphocytes were dying from G_2 by mitotic catastrophe, we used Laser Scanning Cytometry (LSC) to observe polyploid cells resulting from treatment with WP631, and the presence of aberrant mitotic figures was also analyzed under the microscope. As illustrated in Fig. 2A, morphological types of 8n-polyploid Jurkat T cells included cells with both multiple nuclei and unique nucleus containing duplicated DNA. At first glance, some of the multinuclear cells show apoptotic-like phenotypes, such as hypercondensed chromatin aggregates (Fig. 2A). It is worth noting that these cells were polyploid, and they were committed to die during or after mitosis, while p53-dependent apoptosis occurs after G_1, mainly before DNA replication. Under the microscope, most of the untreated cells were morphologically normal and several were observed in prophase, while those treated with WP631 showed many abnormal mitotic figures, including abnormal anaphases, aberrant prophases, uneven chromosome distribution and c-mitosis (see legend to Fig. 2B). The presence of abnormal mitosis was consistent with a cell death mechanism involving mitotic catastrophe.

Jurkat T cells used in our experiments contain a functional p53, and it remained to be determined whether mitotic catastrophe was followed by p53-dependent apoptosis, as reported in some cases (Castedo et al., 2004b; Jordan et al., 1996; Sleiman and Stewart, 2000), yet apoptosis does not appear to be required for the lethal effect of mitotic catastrophe (Roninson et al., 2001). We should recall here that Jurkat T cells, containing functional p53, treated with the IC_{75} for daunorubicin underwent apoptosis from G_1 (Mansilla et al., 2003).

Fig. 2C shows the results of the simultaneous staining of Jurkat T cells with Annexin-V-Fluos, which binds to the membrane of apoptotic cells, and not to normal cells, together with propidium iodide that is taken by both necrotic and apoptotic cells. In this way, we discriminated between the two

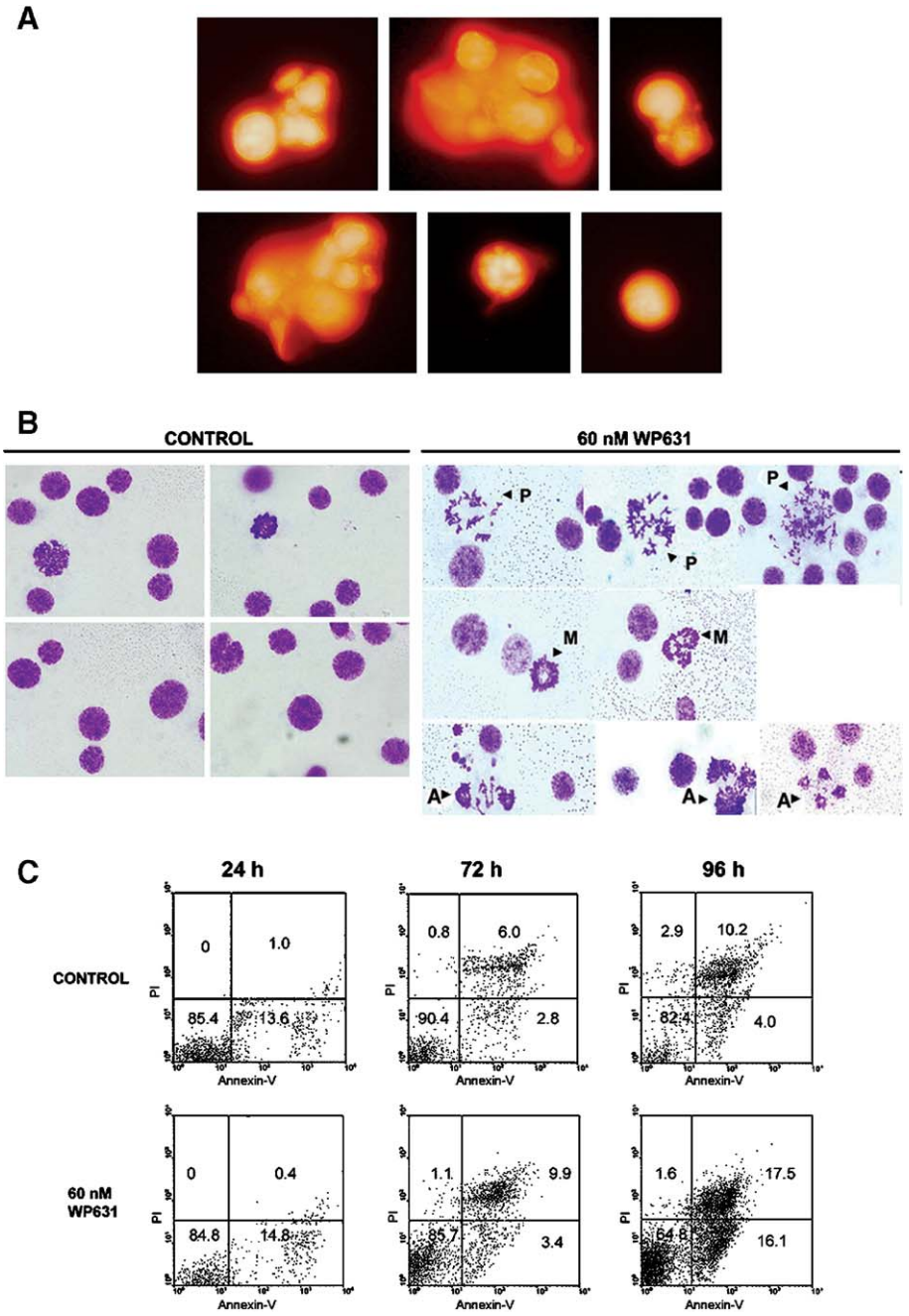

Fig. 2. Mitotic catastrophe in Jurkat T lymphocytes treated with 60 nM WP631 for 72 h. (A) Representative Laser Scanning Cytometry images showing examples of polyploid cells with one or more nuclei stained with propidium iodide. (B) Examples of mitotic figures observed in Jurkat T cells after treatment with 60 nM WP631 compared to control (untreated cells) cells (Leichman's staining; photographed at 1000× magnification). The different mitotic figures are identified in WP631-treated cells as follows: A, multipolar anaphases; M, multipolar metaphases; P, aberrant prophases (C-mitosis). (C) A representative flow cytometry of Jurkat T cells treated with 60 nM WP631, stained with Annexin-V-Fluos and propidium iodide. This analysis differentiates normal (living) cells, which are Annexin-V −/propidium iodide−, from primary necrosis (Annexin-V −/propidium iodide+), apoptosis (Annexin-V +/propidium iodide−) and secondary necrosis (Annexin-V +/propidium iodide+).

cell death mechanisms. After 24 h of continuous treatment, the percentage of surviving cells and of those dying by apoptosis/necrosis were almost the same irrespective of the presence of WP631. Fig. 2C indicates that at 96 h, the time at which WP631-treated cells were undergoing mitotic catastrophe (Fig. 2A), there was a clear preponderance towards apoptotic-like death (Annexin-V positive/propidium iodide negative cells) and secondary necrosis (Annexin-V positive/propidium iodide positive cells). The progressive increase in the percentage of necrosis among WP631-treated cells agrees with the presence of a direct relationship between mitotic catastrophe and cell death through necrosis (Cohen-Jonathan et al., 1999). These results, together with those obtained using other techniques (Figs. 2 and 4 and Table 4), suggest that Jurkat T cells treated with the IC_{75} for WP631 died after entering crisis (M2 stage) by means of mitotic catastrophe. This is in contrast to Jurkat T cells treated with IC_{75} for daunorubicin, which underwent p53-dependent apoptosis (Mansilla et al., 2003).

3.3. The analysis of the transcription levels in Jurkat T lymphocytes exposed to WP631 allowed us to detect changes in the expression of several genes that may determine the final destiny of the cells

We have previously shown WP631 is a powerful transcriptional inhibitor, with an outstanding effect on Sp1-transactivated genes (Mansilla et al., 2004; Martín et al., 1999). To gain insights into the pathways leading to cell death in the presence of WP631, we sought to determine using the Human Oncogene/Tumor Suppressor Atlas Array (BD Biosciences Clontech) the changes in the expression profile of genes that regulate the cell cycle. This includes *p53* and *p21*^{WAF1}, known for their role in the control of G_2 arrest, senescence and mitotic catastrophe (Andreassen et al., 2001; Brown and Attardi, 2005; Bunz et al., 1998; Castedo et al., 2004a; Roninson, 2002).

WP631-treated Jurkat T cells (containing functional p53) showed altered gene transcription patterns, with down-regulation of some genes and up-regulation of others. Fig. 3A shows bivariate scatter plots of the corrected levels of expression of the genes represented in the arrays. A complete data set for all the genes analyzed is available online at the Journal's web page.

Of the 199 genes analyzed, which included 9 constitutively expressed housekeeping genes, 76 changed their expression significantly in the presence of WP631, with 43 being down-regulated and 33 up-regulated. Table 2 lists genes with up- or down-regulated transcription, whose annotated function is related to cell cycle progression, arrest in G_1 or G_2 checkpoints, DNA damage and/or apoptosis (Vermeulen et al., 2003; Vogelstein and Kinzler, 2004). Notably several genes listed in Table 2 presented expression levels very much higher or lower than our chosen 2.5-fold cut-off. For example, *p53* was down-regulated around 17-folds, while the *retinoblastoma* gene (*RB1, Rb*) was up-regulated around 24-folds. However, *n-Ras* was activated 2.51-folds only, at the very edge of what we considered a significant change.

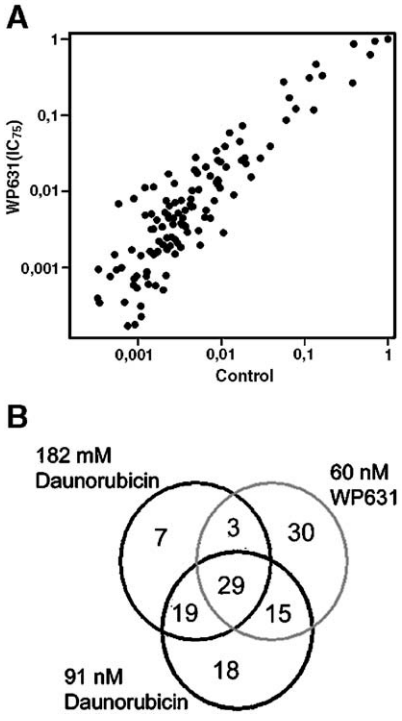

Fig. 3. WP631-induced changes in the expression profiles in Jurkat T lymphocytes. (A) Bivariate scatter plots representing, in logarithmic scale, the expression of the untreated control versus WP631-induced profile levels. (B) Venn diagram showing the number of genes that changed their expression in the presence of 60 nM WP631, compared to those changing with either 182 nM or 91 nM daunorubicin. The complete data set for WP631-treated Jurkat cells is available online. Data for daunorubicin were adapted from Mansilla et al. (2003).

Table 2
A selection of differentially expressed genes in Jurkat T lymphocytes treated with WP631

Genes	60 nM WP631	182 nM daunorubicin [a]	91 nM daunorubicin [a]
c-myc	−[b]	−	+
ATM (ataxia telangiectasia)	=	+	+
p53	−	+	+
MDMX (MDM2-like p53-binding protein)	+	=	−
BRCA-1-associated ring domain 1	−	+	−
p21^{WAF1}	+[c]	=	+
N-Ras	+	=	+
p16^{INK4}	−	+	−
p14^{INK4B}	−	+	+
Cyclin D3	+	=	+
Cyclin E	=	−	+
Cdc25A	=	=	+
RB1(Rb)	+	+	=
130 kDa Rb-associated protein	+	=	−
RBQ-1	=	+	=
RBQ-3	−	+	−
E2F5	−	+	+
CDC-like kinase 2	−	+	+

The table contains several genes implicated previously in checkpoint arrest and apoptosis.
+, up-regulated; −, down-regulated; =, no change.
[a] Data adapted from Mansilla et al. (2003) for the easy of comparison.
[b] As detected by RT-PCR (Fig. 4A).
[c] As detected by qRT-PCR (Fig. 4B).

For comparison purposes, Table 2 also displays the effects of daunorubicin on Jurkat T cells, whose apoptotic effect we had shown to result principally in up-regulation of several cell cycle control genes (Mansilla et al., 2003). Among the genes that are not listed in Table 2, there is the *oncostatin M* (*OSM*) gene, a cytokine that was strongly down-regulated by WP631 (over 200 fold). The *oncostatin M* gene product has been suggested to inhibit DNA synthesis (Klausen et al., 2000). The observed down-regulation of this gene was in keeping with continued DNA synthesis in WP631-treated cells (Fig. 1B).

Given the relevance of several of the genes showing altered expression, including *p53*, *p21*^{WAF1} and *c-myc*, to the development of cell response to antitumour drugs (Elmore et al., 2002; Johnstone et al., 2002; Roninson et al., 2001; Villamarín et al., 2002; Vogelstein et al., 2000), we sought to validate the transcriptional results obtained with the arrays using several complementary techniques. For the easy of comparison, Fig. 4A shows the analysis by semi-quantitative RT-PCR of the effects of WP631 and daunorubicin. Clearly, *c-myc* and *p53*

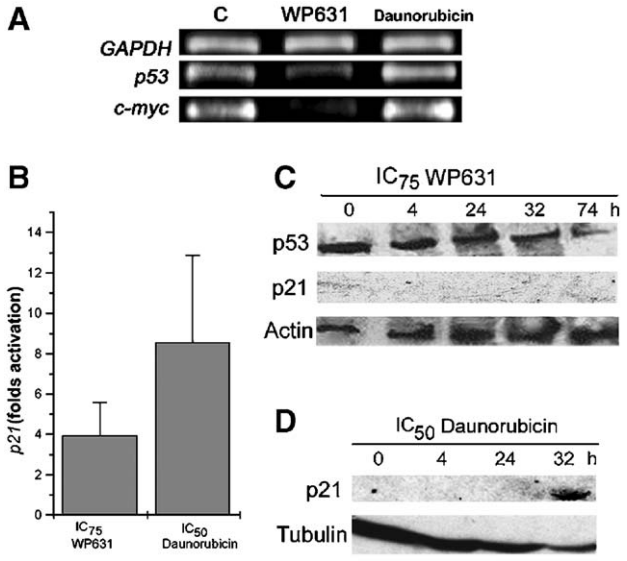

Fig. 4. Verification of altered gene expression in the cDNA array analysis. The relative expression of some selected genes was measured using several techniques. (A) Differential expression of *p53* and *c-myc* assayed by semi-quantitative RT-PCR, with the housekeeping *GAPDH* gene co-amplified as internal control. The effect of the IC_{75} for WP631 is compared with that of the IC_{50} for daunorubicin. (B) Results of a quantitative qRT-PCR used to measure changes in the expression of $p21^{WAF1}$, with the housekeeping *GAPDH* gene used as internal control. This panel represents the changes (folds of activation) of *p21* expression in the presence of WP631, or daunorubicin, compared with *GAPDH* expression (mean±S.D., three experiments). (C) Western blot showing time-dependent reduction in p53 levels, but not in Actin levels, in Jurkat T cells exposed to 60 nM WP631. The p21 protein was not detected under the same experimental conditions. (D) Western blot showing that the $p21^{WAF1}$ protein levels increased abruptly after about 32 h of continuous treatment in the presence of 91 nM (IC_{50}) daunorubicin. Representative Western blot analyses are shown in (C) and (D); two additional experiments yielded similar results.

were down-regulated in the presence of WP631, while *p53* was up-regulated in the presence of daunorubicin, consistent with the presence of p53-dependent apoptosis in Jurkat T cells treated with anthacyclines (da Silva et al., 1996; Mansilla et al., 2003). To validate the effect of WP631 on $p21^{WAF1}$, which changed expression was close to the criteria of exclusion in the array experiments, we used quantitative real-time PCR (qRT-PCR) to compare the actual number of copies of this gene, with those of *GAPDH*. The $p21^{WAF1}$ gene was confirmed to be slightly up-regulated by the IC_{75} for WP631 while with the IC_{50} for daunorubicin (a drug concentration that produces cell senescence (Mansilla et al., 2003)) $p21^{WAF1}$ expression was twice that for WP631 (Fig. 4B).

The p53 protein levels were clearly reduced in the presence of WP631 (Fig. 4C), as well as those of c-myc (Villamarín et al., 2002), coinciding with the moment at which the cells bypass the G_2/M checkpoint stage to enter mitotic catastrophe (Figs. 2 and 4C), and confirming previous results (Villamarín et al., 2002). Various other members of the *myc* family were down-regulated by WP631, above all *L-myc*.

The levels of $p21^{WAF1}$ protein in the Jurkat T cell clone used proved to be too low to be detected by specific antibodies (Western blot in Fig. 4C) in both control and WP631-treated cells. The small changes in $p21^{WAF1}$ gene expression, together with that $p21^{WAF1}$ protein was undetectable, were consistent with the transient stop in G_2 and a no more than momentary senescence-like phenotype (Fig. 1A). Western blot assays showed that p53 protein levels decreased after about 72 h of continuous treatment with the IC_{75} for WP631 (Fig. 4C). The decline in its concentration, which paralleled the overtaking of G_2 arrest, agrees with our previous observations (Villamarín et al., 2002). For the sake of comparison, Fig. 4D shows that the $p21^{WAF1}$ levels increased abruptly in the presence of the IC_{50} for daunorubicin after 32-h treatments, consistent with the cell senescence induced in Jurkat T lymphocytes by low doses of daunorubicin (Mansilla et al., 2003).

The array results showed that the expression of signal transducer and activators of transcription-1 (*STAT1*) gene, a tumour suppressor, did not change significantly in presence of WP631. Since STAT1 is known to induce $p21^{WAF1}$, as an alternative to p53-mediated induction of p21 (Chin et al., 1996), the absence of large changes in $p21^{WAF1}$ levels was consistent with the lack of STAT activation. The time-dependent shortage of p53 protein (Fig. 4C), due to the inhibition of its transcription, may cause a rise in mitotic slippage thus increasing the number of tetraploid cells, as observed (Fig. 2), while the rather low levels of p21 (Fig. 4C) would minimize arrest at the polyploidy checkpoint (Castedo et al., 2004a).

The analysis of the array's data also revealed the up-regulation and down-regulation of several genes of the Wnt signalling pathway by WP631 (Table 3). This pathway is involved in cancer cell maintenance and growth (Reya and Clevers, 2005). Among the genes of the Wnt pathway that were present in our array, a down-regulation of *β-catenin* (over 300-folds) was observed. This may be a result of the direct effect of WP631 on its transcription, or indirectly through the *frizzled* gene product (some homologues of this gene were up-regulated by WP631, see Table 3). Interestingly, β-catenin is known to stimulate *c-myc* expression (Kikuchi, 2000), therefore, down-regulation of β-catenin is consistent with the observed down-regulation of *c-myc*. It is likely that WP631 also inhibited *c-myc* expression directly via interference with Sp1 binding to DNA (Villamarín et al., 2002). Both the effect on the Wnt pathway and on c-myc should result in the observed down-regulation of p53 (Fig. 3A), without the requirement of direct modulation of *p53* expression by WP631. In this way, it is possible to reconcile the observed down-regulation of p53, even though the *p53* promoter lacks Sp1-binding sites (Tuck and Crawford, 1989).

Table 3
Genes of the Wnt signalling pathway that were modulated in Jurkat T lymphocytes by WP631

Gene name	Folds activation/inhibition by WP631
Frizzled homologue 9	2.8
Dishevelled (DVL)+dishevelled 3 (DVL3)	1.9
Dishevelled homologue 1-like protein	1.6
APC (adenomatous polyposis coli protein)	−65.5
β1-catenin (CTNNB)	−28.8
β-catenin	−2.8
c-myc proto-oncogene[a]	−1.4

[a] A target gene transactivated by the APC/β-catenin protein complex.

3.4. Both direct and indirect effects of WP631 on the transcription of hTERT (catalytic subunit of the human telomerase) are in accordance with a transient senescence state in Jurkat T lymphocytes

Although the 'accelerated senescence' observed in the presence of WP631 (Fig. 1) would not require the occurrence of telomere shortening (Shay and Roninson, 2004), we examined whether changes in telomerase activity induced by WP631 may be involved in the transient arrest of Jurkat T cells, perhaps via the effect on *c-myc* transcription. Since the telomerase promoter contains a putative Sp1 binding site, it is also possible that telomerase was inhibited by a direct effect of WP631 on its promoter (Rezler et al., 2003). *C-myc* transcription is regulated by Sp1, and c-myc it is known to cooperate with Sp1 to activate the transcription of *hTERT* (Kyo et al., 2000; Wang et al., 1998). Fig. 5 shows that WP631 inhibited *hTERT* expression activity by about 20% after 4 h of continuous treatment.

We conclude that down-regulation of *c-myc*, and the capacity of WP631 for inhibiting Sp1-transactivated gene expression (Gaidarova and Jiménez, 2002; Mansilla et al., 2004; Martín et al., 1999) might occur together to down-regulate *hTERT* expression.

3.5. Jurkat T cells treated with WP631 die by mitotic catastrophe in the absence of caspase-2 or caspase-3 activities

Caspases are known as executioners of apoptotic cell death. We sought to gain insights into whether Jurkat T cells dying by mitotic catastrophe were using a caspase-dependent route. It has been suggested that suppression of caspase-2 prevents mitotic catastrophe and allows cells to further proceed into the cell cycle beyond metaphase (Castedo et al., 2004b). Neither activation of caspase-2 nor of caspase-3 was detected after treatment with WP631, while in the presence of the IC_{75} for daunorubicin, caspase activities were clearly established (Table 4). This is consistent with our previous report of p53-dependent apoptosis in Jurkat T cells treated with daunorubicin (Mansilla et al., 2003). For WP631-treated cells, high frequency of secondary apoptosis was observed among cells dying by mitotic catastrophe (Fig. 2C), in absence of caspase-2 and caspase-3 activities, suggesting cell death by mechanisms other than by a caspase-dependent way. These results are at variance with previously suggested mechanisms of mitotic catastrophe via caspases activation (Castedo et al., 2004a), yet they are in line with our recent observations in breast carcinoma cells, in which mitotic catastrophe can result in cell death by caspase-dependent and caspase-independent routes (Mansilla et al., 2006). In Jurkat T cells the p53 down-regulation by WP631 may cooperate to induce polyploidy, which did not appear to result in

Table 4
Activation of caspase-2 and caspase-3 in Jurkat-T lymphocytes determined after treatment with WP631 or daunorubicin

	IC_{75} WP631	IC_{50} daunorubicin	IC_{75} daunorubicin
Caspase-2	5.5±3.8	30.3±6.1	100
Caspase-3	6.6±6.7	58.9±3.1	100
Assay time [a]	72 h	48 h	24 h

Caspase activities are presented as relative values, compared to the activity after treatment with the IC_{75} for daunorubicin (scored as 100%). Data are mean±S.D. for 4 experiments.

[a] The enzymatic activities were determined at the indicated times of continuous treatment with the drugs, which correspond to the time point from which cells positive for Trypan blue were observed.

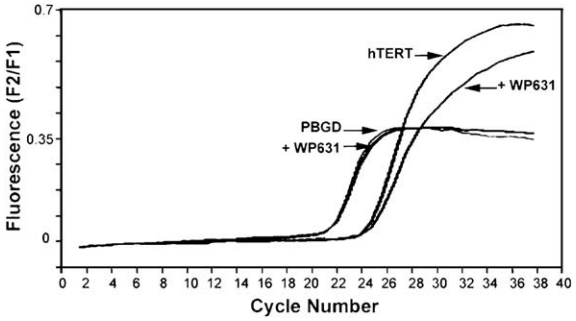

Fig. 5. Representative quantitative real-time PCR experiment of the *hTERT* expression in Jurkat T lymphocytes. The melting curves correspond to quantitative detection of *hTERT* mRNA and *porphobilinogen deaminase (PBGD)* mRNA in the presence of the IC_{75} for WP631, or in its absence. Quantification of *PBGD* mRNA, the levels of which not change significantly in the presence of WP631, was used as a reference for relative *hTERT* mRNA quantification. In the presence of 60 nM WP631, the inhibition of telomerase expression was determined to be about 20% (average of two independent experiments with similar results).

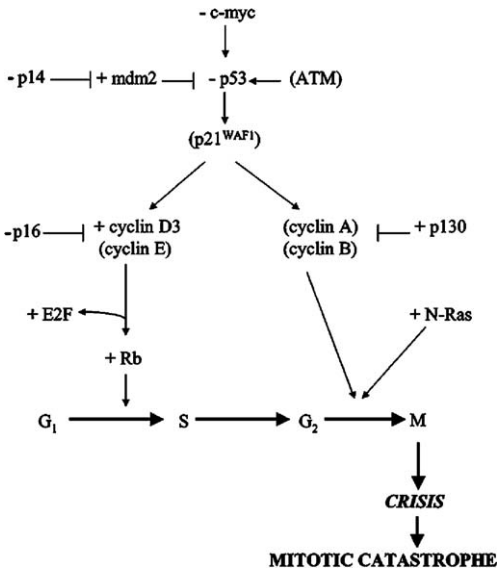

Fig. 6. A tentative pathway used to explain how the transcription profiles of the genes analyzed may participate in the induction of mitotic catastrophe in Jurkat T lymphocytes treated with the IC_{75} for WP631. The pathway was created considering the changes in the transcription profiles obtained by cDNA array analysis (Fig. 3 and Table 2), and the presence of DNA synthesis after 72 of treatment (Fig. 1B), together with the data available on the function of the corresponding gene products on the control of cell cycle, apoptosis, crisis and mitotic catastrophe. Further details and references are provided in the main text. +: up-regulated; −: down-regulated. Parentheses mean that the response of these genes to WP631 was outside the criteria of exclusion in the analysis of the gene profiles (2.5-fold change compared to control), or the genes were not studied in our experiments because they were not present in the array.

survival to the catastrophic event, given that cells died during the days following treatment, as assessed by Trypan blue positive cells within the two days following the withdrawal of the drug.

4. Discussion

Here, we have shown that the down-regulation of p53, together with other induced changes in the transcriptome of Jurkat T lymphocytes, leads to mitotic catastrophe in cells capable of expressing functional p53. In Jurkat T cells, transient senescence and mitotic catastrophe upon WP631 treatment were accompanied by changes in the transcription of several genes, which are involved in G_1 and G_2 checkpoints and cell arrest. Some of them have previously been associated with senescence and mitotic catastrophe (Castedo et al., 2004a; Chang et al., 2002; Johnstone et al., 2002; Shay and Roninson, 2004; Vogelstein et al., 2000). Moreover, both direct and indirect effects of WP631 on the transcription of *hTERT* are in agreement with the transient senescence observed.

Fig. 6 presents a tentative pathway by which WP631 may act in Jurkat T cells, in which the down-regulation of *p53* plays a central role. The p53 protein is known to promote apoptosis and senescence, while it inhibits mitotic catastrophe (Roninson et al., 2001). This pathway considers the up-regulation of *cyclin D*, together with the up-regulation of *Rb*, *E2F* and *N-Ras* (Table 2). It also considers the observation of DNA synthesis in treated cells (Fig. 1B), in keeping with a brief senescence-like phenotype (Fig. 1A) with the cells entering crisis, which resulted in mitotic catastrophe and secondary necrosis (Fig. 3). The down-regulation of *p53*, as well as the low $p21^{WAF1}$ expression (detected by qRT-PCR (Fig. 4B)), would facilitate tetraploidy, in agreement with observations in other cell types (Bunz et al., 1998). Arrest of tetraploid cells has been described to be p21-dependent, yet this protein may not prevent progression into mitotic catastrophe (Andreassen et al., 2001). Cell death in WP631-treated Jurkat T cells (Fig. 2) appeared to occur in a p53-independent way, during or close to the metaphase. In fact, Jurkat T cells treated with WP631 may have unrestricted entrance into mitosis, because in these cells the $p21^{WAF1}$ protein was almost absent after treatment (Fig. 4). Moreover, the absence of caspase activation (Table 4) indicates that mitotic failure and death could occur through routes other than a special (delayed) form of apoptosis.

In summary, the DNA-binding drug WP631 down-regulates *p53* transcription changing Jurkat T lymphocytes from being "apoptotic-competent " (Brown and Attardi, 2005; da Silva et al., 1996; Lotem and Sachs, 1996; Mansilla et al., 2003) to cells committed to die through mitotic catastrophe. WP631 induced crisis (senescence M2 stage) in the presence of low p53 levels, before the cells entered mitotic catastrophe to eventually die in the absence of caspase activity, in keeping with an established link between crisis and mitotic catastrophe (Shay and Wright, 2005). These findings imply that knowing the p53 status of a cancer cell might not suffice to predict the fate of cells treated with some chemotherapeutic drugs. Identification of gene expression patterns in tumour cells, and their modulation by drugs such as WP631 can help to elucidate pathways leading to different cell death mechanisms, representing potential targets in tumours with inactivated p53.

Acknowledgements

This work was financed by grants from the Spanish Ministry of Education and Science (SAF2002-00371 and SAF2005-00551), the FEDER program of the European Community and The Welch Foundation, Houston, TX, and it was carried out within the framework of the Centre de Referencia en Biotecnologia (Generalitat de Catalunya). S.M. was recipient of a doctoral fellowship from the CIRIT, Generalitat de Catalunya.

Appendix A. Supplementary data

Supplementary data associated with this article can be found, in the online version, at doi:10.1016/j.ejphar.2006.04.035.

References

Andreassen, P.R., Lacroix, F.B., Lohez, O.D., Margolis, R.L., 2001. Neither $p21^{WAF1}$ nor 14-3-3σ prevents G2 progression to mitotic catastrophe in human colon carcinoma cells after DNA damage, but $p21^{WAF1}$ induces stable G1 arrest in resulting tetraploid cells. Cancer Res. 61, 7660–7668.

Bataller, M., Portugal, J., 2005. Apoptosis and cell recovery in response to oxidative stress in p53-deficient prostate carcinoma cells. Arch. Biochem. Biophys. 437, 151–158.

Brown, J.M., Attardi, L.D., 2005. The role of apoptosis in cancer development and treatment response. Nat. Rev., Cancer 5, 231–237.

Brown, J.M., Wilson, G., 2003. Apoptosis genes and resistance to cancer therapy: what does the experimental and clinical data tell us? Cancer Biol. Ther. 2, 477–490.

Bunz, F., Dutriaux, A., Lengauer, C., Waldman, T., Zhou, S., Brown, J.P., Sedivy, J.M., Kinzler, K.W., Vogelstein, B., 1998. Requirement for p53 and p21 to sustain G_2 arrest after DNA damage. Science 282, 1497–1501.

Castedo, M., Perfettini, J.L., Roumier, T., Andreau, K., Medema, R., Kroemer, G., 2004a. Cell death by mitotic catastrophe: a molecular definition. Oncogene 23, 2825–2837.

Castedo, M., Perfettini, J.L., Roumier, T., Valent, A., Raslova, H., Yakushijin, K., Horne, D., Feunteun, J., Lenoir, G., Medema, R., Vainchenker, W., Kroemer, G., 2004b. Mitotic catastrophe constitutes a special case of apoptosis whose suppression entails aneuploidy. Oncogene 23, 4362–4370.

Chaires, J.B., Leng, F.F., Przewloka, T., Fokt, I., Ling, Y.H., Perez-Soler, R., Priebe, W., 1997. Structure-based design of a new bisintercalating anthracycline antibiotic. J. Med. Chem. 40, 261–266.

Chang, B.-D., Xuan, Y., Broude, E.V., Zhu, H., Schott, B., Fang, J., Roninson, I. B., 1999. Role of p53 and $p21^{waf1/cip1}$ in senescence-like terminal proliferation arrest induced in human tumor cells by chemotherapeutic drugs. Oncogene 18, 4808–4818.

Chang, B.D., Broude, E.V., Fang, J., Kalinichenko, T.V., Abdryashitov, R., Poole, J.C., Roninson, I.B., 2000. $p21^{Waf1/Cip1/Sdi1}$-induced growth arrest is associated with depletion of mitosis-control proteins and leads to abnormal mitosis and endoreduplication in recovering cells. Oncogene 19, 2165–2170.

Chang, B.-D., Swift, M.E., Shen, M., Fang, J., Broude, E.V., Roninson, I.B., 2002. Molecular determinants of terminal growth arrest induced in tumor cells by a chemotherapeutic agent. Proc. Natl. Acad. Sci. U. S. A. 99, 389–394.

Chin, Y.E., Kitagawa, M., Su, W.C., You, Z.H., Iwamoto, Y., Fu, X.Y., 1996. Cell growth arrest and induction of cyclin-dependent kinase inhibitor $p21^{WAF1/CIP1}$ mediated by STAT1. Science 272, 719–722.

Cohen-Jonathan, E., Bernhard, E.J., McKenna, W.G., 1999. How does radiation kill cells? Curr. Opin. Chem. Biol. 3, 77–83.

da Silva, C.P., de Oliveira, C.R., da Conceiçao, M., de Lima, P., 1996. Apoptosis as a mechanism of cell death induced by different chemotherapeutic drugs in human leukemic T-lymphocytes. Biochem. Pharmacol. 51, 1331–1340.

Dimri, G.P., Lee, X., Basile, G., Acosta, M., Scott, G., Roskelley, C., Medrano, E.E., Linskens, M., Rubelj, I., Pereira-Smith, O., Peacocke, M., Campisi, J., 1995. A biomarker that identifies senescent human cells in culture and in aging skin in vivo. Proc. Natl. Acad. Sci. U. S. A. 92, 9363–9367.

Elmore, L.W., Rehder, C.W., Di, X., McChesney, P.A., Jackson-Cook, C.K., Gewirtz, D.A., Holt, S.E., 2002. Adriamycin-induced senescence in breast tumor cells involves functional p53 and telomere dysfunction. J. Biol. Chem. 277, 35509–35515.

Elmore, L.W., Di, X., Dumur, C., Holt, S.E., Gewirtz, D.A., 2005. Evasion of a single-step, chemotherapy-induced senescence in breast cancer cells: implications for treatment response. Clin. Cancer Res. 11, 2637–2643.

Eom, Y.W., Kim, M.A., Park, S.S., Goo, M.J., Kwon, H.J., Sohn, S., Kim, W.H., Yoon, G., Choi, K.S., 2005. Two distinct modes of cell death induced by doxorubicin: apoptosis and cell death through mitotic catastrophe accompanied by senescence-like phenotype. Oncogene 24, 4765–4777.

Gaidarova, S., Jiménez, S.A., 2002. Inhibition of basal and transforming growth factor-β-induced stimulation of COL1A1 transcription by the DNA intercalators, mitoxantrone and WP631, in cultured human dermal fibroblasts. J. Biol. Chem. 277, 38737–38745.

Gatti, L., Beretta, G.L., Carenini, N., Corna, E., Zunino, F., Perego, P., 2004. Gene expression profiles in the cellular response to a multinuclear platinum complex. Cell. Mol. Life Sci. 61, 973–981.

Huang, X., Tran, T., Zhang, L., Hatcher, R., Zhang, P., 2005. DNA damage-induced mitotic catastrophe is mediated by the Chk1-dependent mitotic exit DNA damage checkpoint. Proc. Natl. Acad. Sci. U. S. A. 102, 1065–1070.

Inge, T.H., Casson, L.K., Priebe, W., Trent, J.O., Georgeson, K.E., Miller, D.M., Bates, P.J., 2002. Importance of Sp1 consensus motifs in the MYCN promoter. Surgery 132, 232–238.

Johnstone, R.W., Ruefli, A.A., Lowe, S.W., 2002. Apoptosis. A link between cancer genetics and chemotherapy. Cell 108, 153–164.

Jordan, M.A., Wendell, K., Gardiner, S., Derry, W.B., Copp, H., Wilson, L., 1996. Mitotic block induced in HeLa cells by low concentrations of paclitaxel (Taxol) results in abnormal mitotic exit and apoptotic cell death. Cancer Res. 56, 816–825.

Kikuchi, A., 2000. Regulation of β-catenin signaling in the Wnt pathway. Biochem. Biophys. Res. Commun. 268, 243–248.

Klausen, P., Pedersen, L., Jurlander, J., Baumann, H., 2000. Oncostatin M and interleukin 6 inhibit cell cycle progression by prevention of $p27^{kip1}$ degradation in HepG2 cells. Oncogene 19, 3675–3683.

Kyo, S., Takakura, M., Taira, T., Kanaya, T., Itoh, H., Yutsudo, M., Ariga, H., Inoue, M., 2000. Sp1 cooperates with c-Myc to activate transcription of the human telomerase reverse transcriptase gene (hTERT). Nucleic Acids Res. 28, 669–677.

Lock, R.B., Stribinskiene, L., 1996. Dual modes of death induced by etoposide in human epithelial tumor cells allow Bcl-2 to inhibit apoptosis without affecting clonogenic survival. Cancer Res. 56, 4006–4012.

Lotem, J., Sachs, L., 1996. Control of apoptosis in hematopoiesis and leukemia by cytokines, tumor suppressor and oncogenes. Leukemia 10, 925–931.

Lowe, S.W., Bodis, S., McClatchey, A., Remington, L., Ruley, H.E., Fisher, D.E., Housman, D.E., Jacks, T., 1994. p53 status and the efficacy of cancer therapy in vivo. Science 266, 807–810.

MacKenzie, K.L., Franco, S., May, C., Sadelain, M., Moore, M.A., 2000. Mass cultured human fibroblasts overexpressing hTERT encounter a growth crisis following an extended period of proliferation. Exp. Cell Res. 259, 336–350.

Mansilla, S., Piña, B., Portugal, J., 2003. Daunorubicin-induced variations in gene transcription: commitment to proliferation arrest, senescence and apoptosis. Biochem. J. 372, 703–711.

Mansilla, S., Priebe, W., Portugal, J., 2004. Sp1-targeted inhibition of gene transcription by WP631 in transfected lymphocytes. Biochemistry 43, 7584–7592.

Mansilla, S., Priebe, W., Portugal, J., 2006. Mitotic catastrophe results in cell death by caspase-dependent and caspase-independent mechanisms. Cell Cycle 5, 53–60.

Martín, B., Vaquero, A., Priebe, W., Portugal, J., 1999. Bisanthracycline WP631 inhibits basal and Sp1-activated transcription initiation in vitro. Nucleic Acids Res. 27, 3402–3409.

Minemoto, Y., Uchida, S., Ohtsubo, M., Shimura, M., Sasagawa, T., Hirata, M., Nakagama, H., Ishizaka, Y., Yamashita, K., 2003. Loss of p53 induces M-phase retardation following G2 DNA damage checkpoint abrogation. Arch. Biochem. Biophys. 412, 13–19.

Nitta, M., Kobayashi, O., Honda, S., Hirota, T., Kuninaka, S., Marumoto, T., Ushio, Y., Saya, H., 2004. Spindle checkpoint function is required for mitotic catastrophe induced by DNA-damaging agents. Oncogene 23, 6548–6558.

Perego, P., Corna, E., Cesare, M.D., Gatti, L., Polizzi, D., Pratesi, G., Supino, R., Zunino, F., 2001. Role of apoptosis and apoptosis-related genes in cellular response and antitumor efficacy of anthracyclines. Curr. Med. Chem. 8, 31–37.

Pozarowski, P., Huang, X., Gong, R.W., Priebe, W., Darzynkiewicz, Z., 2004. Simple, semiautomatic assay of cytostatic and cytotoxic effects of antitumor drugs by laser scanning cytometry: effects of the bis-intercalator WP631 on growth and cell cycle of T-24 cells. Cytometry 57A, 113–119.

Qureshi, H.Y., Sylvester, J., Mabrouk, M.E., Zafarullah, M., 2005. TGF-β-induced expression of tissue inhibitor of metalloproteinases-3 gene in chondrocytes is mediated by extracellular signal-regulated kinase pathway and Sp1 transcription factor. J. Cell. Physiol. 203, 345–352.

Reya, T., Clevers, H., 2005. Wnt signalling in stem cells and cancer. Nature 434, 843–850.

Rezler, E.M., Bearss, D.J., Hurley, L.H., 2003. Telomere inhibition and telomere disruption as processes for drug targeting. Annu. Rev. Pharmacol. Toxicol. 43, 359–379.

Roninson, I.B., 2002. Tumor senescence as a determinant of drug response in vivo. Drug Resist. Updat. 5, 204–208.

Roninson, I.B., 2003. Tumor cell senescence in cancer treatment. Cancer Res. 63, 2705–2715.

Roninson, I.B., Broude, E.V., Chang, B.-D., 2001. If not apoptosis, then what? Treatment-induced senescence and mitotic catastrophe in tumor cells. Drug Resist. Updat. 4, 303–313.

Shay, J.W., Roninson, I.B., 2004. Hallmarks of senescence in carcinogenesis and cancer therapy. Oncogene 23, 2919–2933.

Shay, J.W., Wright, W.E., 2005. Senescence and immortalization: role of telomeres and telomerase. Carcinogenesis 26, 867–874.

Sleiman, R.J., Stewart, B.W., 2000. Early caspase activation in leukemic cells subject to etoposide-induced G2-M arrest: evidence of commitment to apoptosis rather than mitotic cell death. Clin. Cancer Res. 6, 3756–3765.

Sleiman, R.J., Catchpoole, D.R., Stewart, B.W., 1998. Drug-induced death of leukaemic cells after G2/M arrest: higher order DNA fragmentation as an indicator of mechanism. Br. J. Cancer 77, 40–50.

Torres, K., Horwitz, S.B., 1998. Mechanisms of Taxol-induced cell death are concentration dependent. Cancer Res. 58, 3620–3626.

Tuck, S.P., Crawford, L., 1989. Characterization of the human *p53* gene promoter. Mol. Cell. Biol. 9, 2163–2172.

Vermes, I., Haanen, C., Steffens-Nakken, H., Reutelingsperger, C., 1995. A novel assay for apoptosis. Flow cytometric detection of phosphatidylserine expression on early apoptotic cells using fluorescein labelled Annexin V. J. Immunol. Methods 184, 39–51.

Vermeulen, K., Berneman, Z.N., Van Bockstaele, D.R., 2003. Cell cycle and apoptosis. Cell Prolif. 36, 165–175.

Villamarín, S., Ferrer-Miralles, N., Mansilla, S., Priebe, W., Portugal, J., 2002. Induction of G2/M arrest and inhibition of *c-myc* and *p53* transcription by WP631 in Jurkat T cells. Biochem. Pharmacol. 63, 1251–1258.

Villamarín, S., Mansilla, S., Ferrer-Miralles, N., Priebe, W., Portugal, J., 2003. A comparative analysis of the time-dependent antiproliferative effects of daunorubicin and WP631. Eur. J. Biochem. 270, 764–770.

Vogelstein, B., Kinzler, K.W., 2004. Cancer genes and the pathways they control. Nat. Med. 10, 789–799.

Vogelstein, B., Lane, D., Levine, A.J., 2000. Surfing the p53 network. Nature 408, 307–310.

Wang, J., Xie, L.Y., Allan, S., Beach, D., Hannon, G.J., 1998. Myc activates telomerase. Genes Dev. 12, 1769–1774.

Weller, M., 1998. Predicting response to cancer chemotherapy: the role of p53. Cell Tissue Res. 292, 435–445.

Yashige, H., Horiike, S., Taniwaki, M., Misawa, S., Abe, T., 1999. Micronuclei and nuclear abnormalities observed in erythroblasts in myelodysplastic syndromes and in de novo acute leukemia after treatment. Acta Haematol. 101, 32–40.

Zhivotovsky, B., 2004. Apoptosis, necrosis and between. Cell Cycle 3, 64–66.